ORIGINAL RESEARCH

Genetic Control of Fatty Acid β-Oxidation in Chronic Obstructive Pulmonary Disease

Zhiqiang Jiang[1], Nelson H. Knudsen[2,3], Gang Wang[4], Weiliang Qiu[1], Zun Zar Chi Naing[1], Yan Bai[5], Xingbin Ai[5], Chih-Hao Lee[2,3], and Xiaobo Zhou[1,5]

[1]Channing Division of Network Medicine and [5]Division of Pulmonary and Critical Care Medicine, Department of Medicine, Brigham and Women's Hospital and Harvard Medical School, Departments of [2]Genetics and Complex Diseases, and [3]Nutrition, Division of Biological Sciences, Harvard T. H. Chan School of Public Health, Boston, Massachusetts, and [4]Department of Cardiology, Boston Children's Hospital, Boston, Massachusetts

ORCID ID: 0000-0002-7127-2869 (X.Z.).

Abstract

Bioenergetics homeostasis is important for cells to sustain normal functions and defend against injury. The genetic controls of bioenergetics homeostasis, especially lipid metabolism, remain poorly understood in chronic obstructive pulmonary disease (COPD), the third leading cause of death in the world. Additionally, the biological function of most of the susceptibility genes identified from genome-wide association studies (GWASs) in COPD remains unclear. Here, we aimed to address (*1*) how fatty acid oxidation (FAO), specifically β-oxidation, a key lipid metabolism pathway that provides energy to cells, contributes to cigarette smoke (CS)-induced COPD; and (*2*) whether—and if so, how—FAM13A (family with sequence similarity 13 member A), a well-replicated COPD GWAS gene, modulates the FAO pathway. We demonstrated that CS induced expression of carnitine palmitoyltransferase 1A (CPT1A), a key mitochondrial enzyme for the FAO pathway, thereby enhancing FAO. Pharmacological inhibition of FAO by etomoxir blunted CS-induced reactive oxygen species accumulation and cell death in lung epithelial cells. FAM13A promoted FAO, possibly by interacting with and activating sirutin 1, and increasing expression of CPT1A. Furthermore, CS-induced cell death was reduced in lungs from *Fam13a*$^{-/-}$ mice. Our results suggest that FAM13A, the COPD GWAS gene, shapes the cellular metabolic response to CS exposure by promoting the FAO pathway, which may contribute to COPD development.

Keywords: cigarette smoke; mitochondria; fatty acid β-oxidation; *FAM13A*; *CPT1A*

Clinical Relevance

Genome-wide association studies (GWAS) have been very successful in discovering genetic loci statistically associated with complex traits. However, understanding the biological function and molecular mechanisms of candidate genes within GWAS loci is an ongoing challenge. In this work, we connected a novel chronic obstructive pulmonary disease GWAS gene, FAM13A, with an important lipid metabolism pathway, fatty acid β-oxidation, at molecular levels in cellular and murine models. This novel genetic link between emphysema and lipid metabolism may open a new avenue for the treatment of chronic obstructive pulmonary disease, given the wide spectrum of pharmacological inhibitors of the fatty acid β-oxidation pathway.

Maintenance of cellular energy homeostasis is important under many physiological and pathological conditions that may well extend beyond metabolic diseases. This balance of cellular energy has not yet been well studied in lung diseases, including chronic obstructive pulmonary disease (COPD), the third leading cause of death in the United States (1). COPD is a complex disease that is strongly influenced by both cigarette smoking and genetic predisposition. The known pathogenesis of

(Received in original form August 31, 2016; accepted in final form January 31, 2017)

This work was supported by National Institutes of Health grants R01HL112176 and R33HL114305 (X.Z.).

Author contributions: Z.J. and X.Z. designed the study. Z.J. and Z.Z.C.N. performed all experimental work. Z.J., W.Q., and X.Z completed the statistical analysis of all results. N.H.K. and C.-H.L. oversaw the β-oxidation rate measurements. G.W. helped to interpret the Seahorse measurements. Y.B. and X.A. provided human lung slices. Z.J. and X.Z. wrote the manuscript.

Correspondence and requests for reprints should be addressed to Xiaobo Zhou, Ph.D., 221 Longwood Avenue EBRC620c, Channing Division of Network Medicine, Brigham and Women's Hospital, Boston, MA 02115. E-mail: xiaobo.zhou@channing.harvard.edu

This article has an online supplement, which is accessible from this issue's table of contents at www.atsjournals.org

Am J Respir Cell Mol Biol Vol 56, Iss 6, pp 738–748, Jun 2017

Originally Published in Press as DOI: 10.1165/rcmb.2016-0282OC February 15, 2017
Internet address: www.atsjournals.org

COPD is highly complex and includes an imbalance between proteinase and antiproteinase (2), oxidative stress (3), inflammation (4), epithelial cell death (5, 6), and mitochondrial dysfunction (7). Recently, disrupted lipid metabolism was detected in patients with COPD (8–11) as well as in a cigarette smoke (CS)-induced emphysema murine model (12), suggesting a dysregulation of lipid metabolism during COPD development.

Fatty acids (FAs), as one of the main types of lipids, provide energy for many organisms through oxidation. The three types of FA oxidative degradation processes that occur in cells, namely, α-, β-, and ω-oxidation, take place in specialized subcellular structures, the mitochondria and peroxisomes (13, 14). Most FAs are catabolized by FA β-oxidation (FAO) inside mitochondria where even-numbered saturated FAs are oxidized, thus providing acetyl-coenzyme A (acetyl-CoA) as a substrate for the citric acid cycle. This process consists of two steps: first, long-chain acetyl-CoA is transported from the cytosol into mitochondria by carnitine palmitoyltransferase (mainly CPT1); second, fatty acetyl-CoA is catalyzed by trifunctional enzymes inside the mitochondria. Through FAO, adenosine triphosphates (ATPs) are produced, accompanied by reactive oxygen species (ROS) (15).

Under physiological conditions, glucose is generally the main energy source in lung epithelial cells. Acute CS exposure was shown to induce a switch from glucose to lipid as the main energy source and increase FAO in distal lung epithelial cells, likely by increasing CPT1A activity (16), thereby generating ATP. However, whether—and if so, how—FAO contributes to CS-induced emphysema remains unexplored.

From genome-wide association studies (GWASs), several genetic loci have been unequivocally associated with COPD susceptibility in multiple cohorts. Among these loci, the *FAM13A* (family with sequence similarity 13 member A) locus at 4q24 (17, 18) repeatedly showed a strong association with COPD (19), but the molecular mechanisms and the biological function of FAM13A in lungs are largely unknown (20). Previously, we demonstrated increased expression of FAM13A in human COPD lungs compared with ex-smoker controls, and that *Fam13a*$^{-/-}$ mice are resistant to CS-induced emphysema, which might be linked to increased levels of β-catenin and cell proliferation in the lungs of *Fam13a*$^{-/-}$ mice (21). Furthermore, the FAM13A locus has also been consistently linked with metabolic diseases (22, 23), suggesting plausible roles of FAM13A in regulating energy homeostasis and metabolism.

In this work, we set out to understand the bioenergetics changes that occur in lung epithelial cells under CS exposure and to explore the roles of FAO in CS-induced lung injury, which is modified by the COPD GWAS gene FAM13A. By examining the results of CS exposure in murine and cellular models, we demonstrated that FAO mediates CS-induced ROS production and cell death, while FAM13A promotes FAO, possibly by increasing the expression of CPT1A, the key rate-limiting enzyme in FAO.

Materials and Methods

A full description of the experimental procedures used in this work is available in the online supplement.

Cell lines, Plasmids, Mice, and *In Vivo* CS Exposure

All cells were purchased from ATCC (American Type Culture Collection, Manassas, VA). Human bronchial epithelial (16HBE) cells were cultured in Eagle's minimal essential medium. Human embryonic kidney (HEK) 293 cells were cultured in Dulbecco's modified Eagle's medium (DMEM) supplemented with 10% fetal bovine serum, penicillin (50 U/ml), and streptomycin (50 μg/ml). *Mycoplasma* was tested routinely using the Mycoalert Detection Kit (LT07-218; Lonza, Hopkinton, MA) in cells used in this study. 16HBE cells stably infected with control nontargeting short hairpin RNA (shRNA) or human FAM13A shRNA were established previously (21). Full-length human FAM13A (NP_001252507.1) was cloned as described previously (21).

Fam13a$^{-/-}$ mice generated in a C57BL/6J background and littermate wild-type mice were exposed to CS as described previously (21). At the end of the exposure period, the mice were killed by CO_2 narcosis and cervical dislocation, and the lungs were removed. Lung sections from mice exposed to CS or air for 1 month were assessed for cell death by terminal deoxynucleotidyl transferase dUTP nick end labeling (TUNEL) staining. Primary lung alveolar epithelial cells isolated from mice that were exposed to air or CS for 5 months were assessed for mitochondrial respiration via Seahorse measurements (Seahorse Bioscience, North Billerica, MA). All mice were housed in the animal facility of Harvard Medical School under a 12-h light/12-h dark cycle.

Measurements of Mitochondrial Respiration

We used an Extracellular Flux Analyzer (Seahorse Bioscience) to measure the oxygen consumption rate (OCR), an indicator of mitochondrial respiration, in either 16HBE cells or primary murine distal lung epithelial cells in a 24-well plate. Briefly, cells were seeded directly into XF24 plates and mitochondrial respiration was measured in XF assay medium modified DMEM (Seahorse Bioscience) supplemented with D-glucose (25 mM) and pyruvate (1 mM). 16HBE cells were seeded at a density of 3×10^4 cells/well and OCR was measured using the MitoStress program. During the assay, oligomycin (2 μM), carbonyl cyanide-4-(trifluoromethoxy)phenylhydrazone (2 μM), and actinomycin/rotenone (1 μM of each) were sequentially added into each well to measure ATP production, maximum respiration, and proton leak (complex I driven), respectively. Primary distal lung epithelial cells were seeded into plates that were precoated with CellTak (Corning, Bedford, MA) at a density of 1×10^5 cells/well, followed by OCR measurements using the same program employed for the 16HBE cells. During the assay, oligomycin (4 μM), carbonyl cyanide-4-(trifluoromethoxy)phenylhydrazone (4 μM), and actinomycin/rotenone (2 μM of each) were added into each well sequentially.

Measurements of β-oxidation

FAO was measured in 16HBE cells stably infected with FAM13A shRNA or overexpressing FLAG-tagged human FAM13A using previously described methods (21). 16HBE cells were seeded in 24-well plates and incubated for 24 h with labeling medium (400 μl 1 g/L DMEM supplemented with 2% FA-free BSA [Gemini Bio Products, West Sacramento, CA], 0.25 mM carnitine [Sigma-Aldrich,

Natick, MA], and 2 μCi ^{3}H-palmitic acid [American Radiolabeled Chemicals, St. Louis, MO]). After incubation, the supernatant sample was mixed with 10% trichloroacetic acid (Sigma-Aldrich) for 15 min and centrifuged at full speed for 10 min. The supernatant was then mixed with 5% trichloroacetic acid and BSA, incubated at room temperature for 15 min, and extracted using chloroform:methanol (2:1) and 2 M potassium chloride:hydrochloride. Then, the supernatant was mixed with 5 ml of EcoLume Liquid Scintillation Cocktail (MP Biomedicals, Santa Ana, CA). The count per minute was measured for 5 min for each sample. The count-per-minute readings from cell-free medium incubated with ^{3}H-labeled medium were used as background to correct all samples. Final results were obtained after normalization using the protein concentration.

Statistical Method

We tested the data for normality before performing unpaired Student's *t* tests. Any data that were not normally distributed were analyzed using a nonparametric test. However, most of the *in vitro* data with a limited sample size showed a normal distribution. We then performed unpaired *t* tests with equal variance to compare the impacts of genotype and treatment under each given condition. Details regarding the statistical analysis are provided in the online supplement.

Results

CS Promotes FAO

To determine the impact of CS exposure on cellular mitochondrial respiration and cellular energy homeostasis, we exposed 16HBE cells, an immortalized HBE cell line, to 3% CS extracts (CSEs) for 12 h before measuring the OCR using the Seahorse method. Basal and maximum mitochondrial respiration increased by 50% and 100%, respectively, after CS treatment in 16HBE cells, accompanied by 60% increased ATP production after CS treatment (Figures 1A–1E). Furthermore, such CS-induced elevations in mitochondrial respiration were attenuated by etomoxir (Eto, 50 μM) (Figure 1), which inhibits CPT1A, the rate-limiting enzyme for FAO (Figure E1A in the online supplement). In addition, genetically silencing CPT1A by small interfering RNA (siRNA) attenuated the induction of maximum mitochondrial respiration by CS in 16HBE cells (Figure E1B). These results suggested that CS may enhance FAO and promote mitochondrial respiration in HBE cells. This was further confirmed by a 32% increase of FAO by direct measurements (24) in 16HBE cells exposed to CS (Figure 1F). Furthermore, expression of CPT1A (25) increased by 4-fold in 16HBE cells exposed to 3% CS for 12 h (Figure 1G), consistent with a previous report (16). In sum, CS exposure promoted FAO and increased mitochondrial respiration in HBE cells.

FAO Mediates CS-Induced ROS Production and Cell Death

Given that mitochondrial respiration increased in bronchial epithelial cells after smoke exposure, we next assessed the impact of elevated FAO on CS-induced cell death and accumulation of ROS (5, 6, 26), which contribute to emphysema development. Surprisingly, cells cotreated with Eto (50 μM) and CS showed improved cell viability (from 55% to 79%) compared with cells treated with CS alone (Figure 2A). Similarly, genetic inhibition of FAO by CPT1A siRNA also significantly improved cell viability from 56% to 76% (Figure 2B), suggesting that a lower FAO rate is beneficial in preventing CS-induced cell death. Additionally, inhibition of FAO by Eto reduced CSE-induced mitochondrial and intracellular ROS production (Figures 2C and 2D). These results suggested that FAO mediates CS-induced cell death and mitochondrial-derived ROS accumulation. Consistently, the percentage of TUNEL-positive cells (indicative of cell death) was reduced from 4% to 0.2% in human lung slices (27) cotreated with Eto (100 μM) and 6% CSE for 24 h compared with CSE treatment alone (Figures 2E and 2F).

To address the contribution of FAO to CS-induced cell death *in vivo*, we injected Eto intraperitoneally into C57BL/6 mice that were exposed to CS for 1 month, and then assessed cell death by TUNEL staining. The choice of 1 month of CS exposure was based on a previous report that CS-induced cell death was significantly increased after 1 month of CS exposure (28). In our assays, the number of TUNEL-positive cells increased 20-fold after 1 month of CS exposure. However, cell death was greatly attenuated in lungs from CS-exposed mice cotreated with Eto (25 mg/kg, every other day) compared with mice exposed to CS alone (Figures 2G and 2H). Therefore, FAO mediates CS-induced cell death *in vitro* and *in vivo*.

FAM13A Promotes Mitochondrial Respiration by Enhancing FAO in HBE Cells

We then tested whether mitochondrial respiration is regulated by FAM13A. First, as indicated by the OCR, the maximum mitochondrial respiration was reduced by half and basal respiration showed a trend toward reduced OCR after FAM13A silencing in 16HBE cells (Figures 3A, 3B, and E2). Second, primary distal lung epithelial cells (mainly alveolar type II cells [>70%; Figure E3]) isolated from *Fam13a*$^{-/-}$ mice also showed impaired maximum respiration compared with those from *Fam13a*$^{+/+}$ mice (Figures 3C, 3D, and E4), suggesting that FAM13A promotes mitochondrial respiration in primary lung epithelial cells. Furthermore, supplementing cells with sufficient palmitate acid as fuel to promote FAO increased the OCR in primary lung epithelial cells from *Fam13a*$^{+/+}$ mice, but not in those from *Fam13a*$^{-/-}$ mice (Figure E5A). Similar results were also obtained in human 16HBE cells depleted of FAM13A (Figure E5B). These results suggested that FAM13A increases mitochondrial respiration by promoting FAO. Additionally, direct measurements on FAO demonstrated a 50% reduction after depletion of FAM13A and a 48% increase with overexpression of FAM13A in 16HBE cells (Figure 3E).

To determine the possible mechanism by which FAM13A regulates FAO, we measured the expression of different enzymes related to FAO in murine lungs from *Fam13a*$^{+/+}$ and *Fam13a*$^{-/-}$ mice that had been exposed to chronic CS for 6 months, at which point only the *Fam13a*$^{+/+}$ mice showed airspace enlargement (21). Among four genes we measured (*Acadl* [ACADL acyl-CoA dehydrogenase, long chain], *Cpt1a*, *Mcat* [Malonyl CoA:ACP acyltransferase], and *Cd36* [cluster of differentiation 36]), CPT1A mRNA levels showed a significant reduction (by two-thirds) in *Fam13a*$^{-/-}$ lungs compared with treatment-matched *Fam13a*$^{+/+}$ mice (Figure E6A). Reduced expression of CPT1A was also detected in 16HBE cells silenced for FAM13A (Figure E6B). These results indicated that FAM13A may increase expression of CPT1A, the key

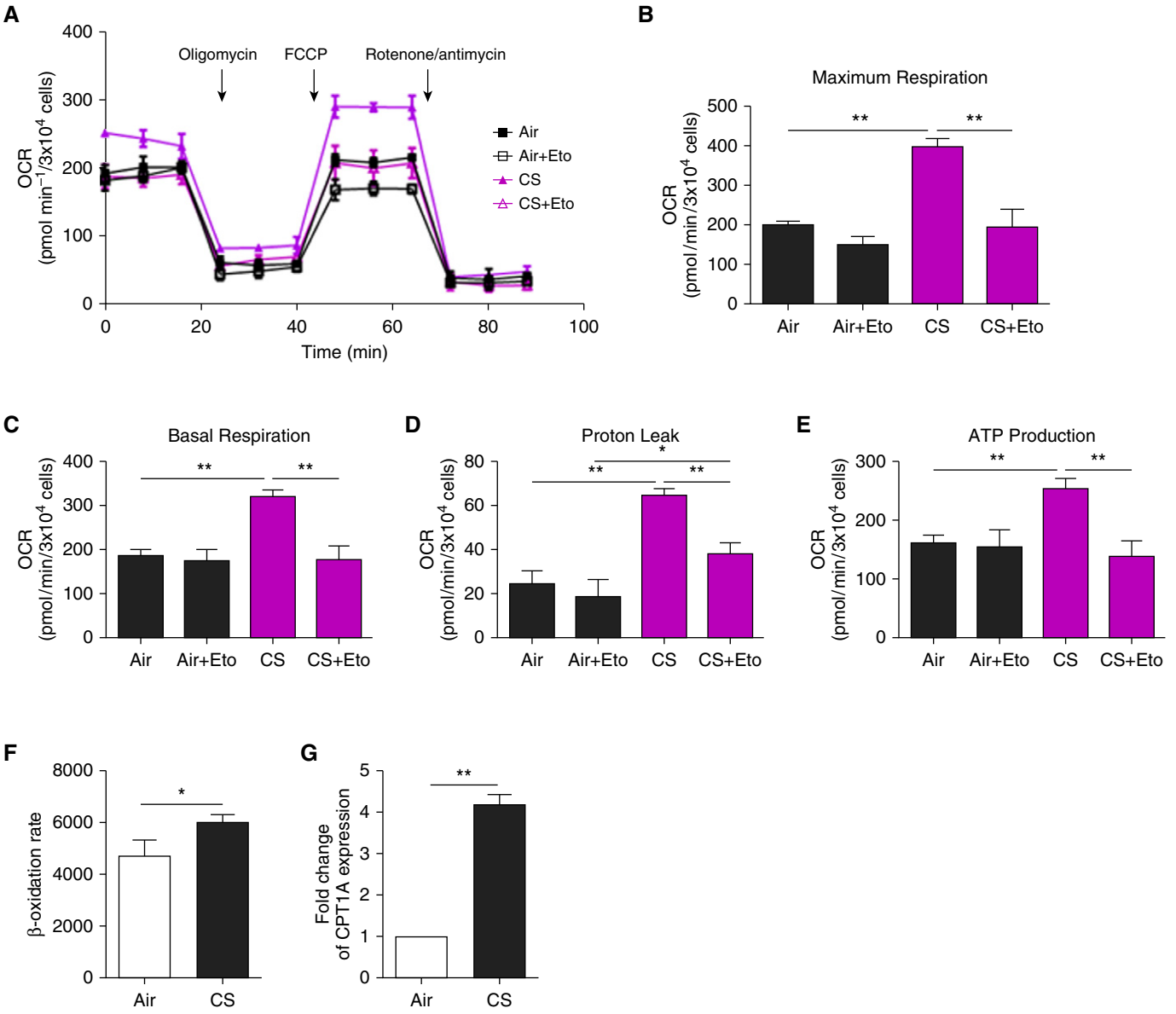

Figure 1. Cigarette smoke (CS) activates fatty acid β-oxidation (FAO) in human bronchial epithelial cells. (*A*) Oxygen consumption rate (OCR) measured by Seahorse assay in human bronchial epithelial (16HBE) cells exposed to CS with/without the β-oxidation inhibitor etomoxir (Eto). (*B*) Maximum mitochondrial respiration, (*C*) basal respiration, (*D*) proton leak, and (*E*) ATP production measurements in *A*. Means ± SD are from triplicate wells. (*F*) Measurements of FAO in16HBE cells treated with CS. Means ± SD from triplicate wells representative of two independent repeats. (*G*) Measurements of CPT1A mRNA levels in 16HBE cells treated with CS. $^{*}P < 0.05$ and $^{**}P < 0.01$ by unpaired Student's *t* test. Means ± SD from triplicate wells in three independent repeats. FCCP, carbonyl cyanide-4-(trifluoromethoxy)phenylhydrazone.

rate-limiting enzyme in FAO. Furthermore, FAO increased 2-fold after overexpression of FAM13A but was reduced by 75% in 16HBE cells after CPT1A silencing regardless of overexpression of FAM13A, suggesting that FAM13A promotes FAO through CPT1A (Figure 3F). Consistently, overexpression of FAM13A increased mitochondria respiration, which was attenuated by CPT1A silencing in 16HBE cells (Figure E7), indicating that FAM13A promotes oxygen consumption, likely through CPT1A.

It is noteworthy that the glycolysis rate, as measured by the Seahorse extracellular acidification rate, showed no difference in 16HBE cells overexpressing FAM13A. The extracellular acidification rates obtained in primary distal lung epithelial cells isolated from *Fam13a*$^{-/-}$ cells are also comparable to those determined in cells from *Fam13a*$^{+/+}$ mice (Figure E8), suggesting minimal regulation of FAM13A during glycolysis in airway epithelial cells.

FAM13A Interacts with Sirtuin 1 and Promotes FAO through CPT1A

Previously, we demonstrated that FAM13A promotes the degradation of β-catenin, the key molecular mediator in the canonical

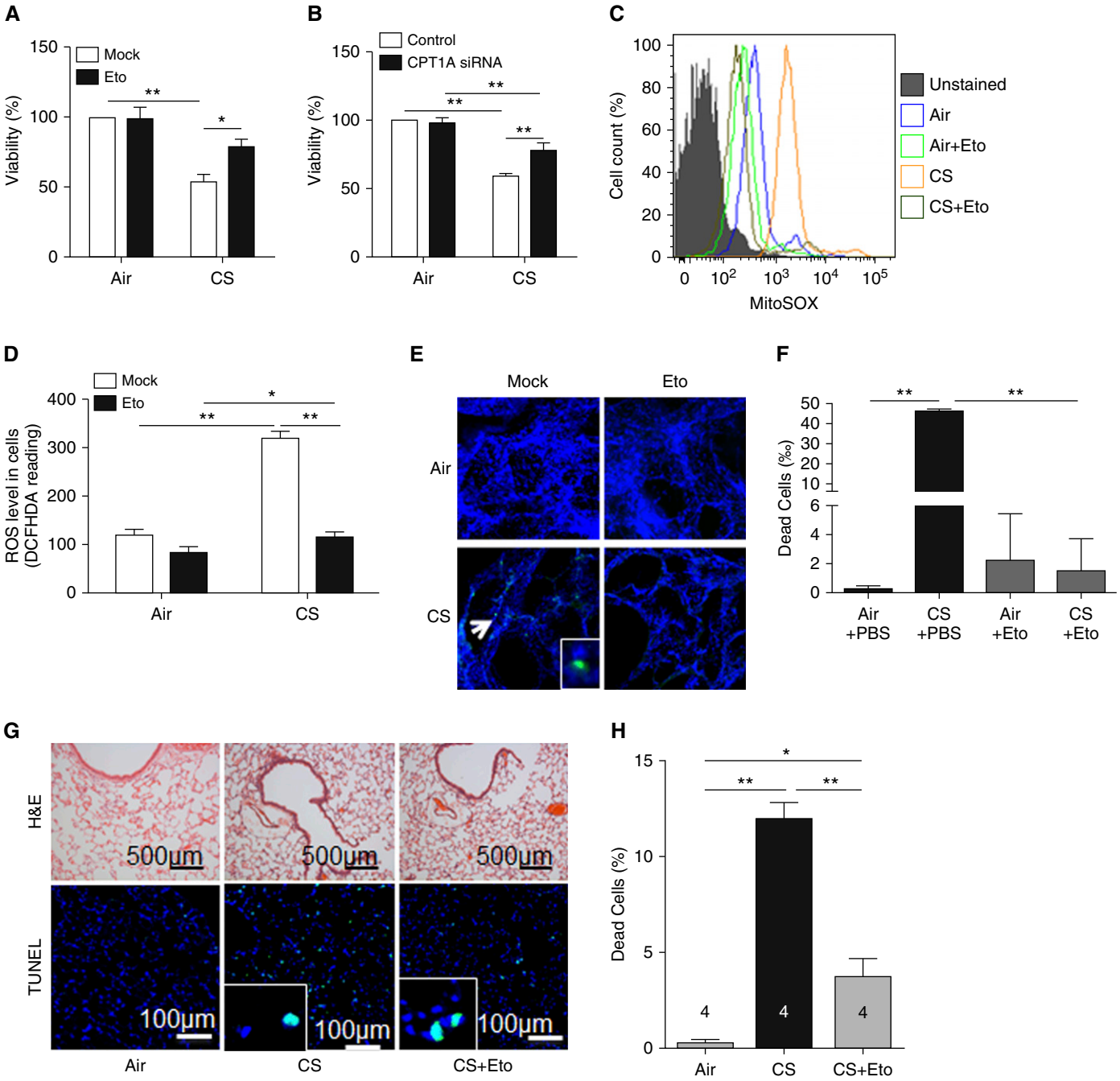

Figure 2. FAO mediates CS-induced cell death and accumulation of mitochondrial-derived reactive oxygen species (ROS). (*A*) Cell viability measurements in 16HBE cells treated with CS and Eto. (*B*) Cell viability measurements in 16HBE cells transfected with CPT1A small interfering RNA (siRNA) and treated with CS. (*C*) Mitochondria-derived ROS indicated by MitoSOX staining in 16HBE cells by flow-cytometry analysis. (*D*) Intracellular ROS measurements in 16HBE cells by dichloro-dihydro-fluorescein diacetate (DCFH-DA) staining. Eto: 50 μM. CS treatment in *A–E*: 3% CS extract (CSE) for 12 h. Terminal deoxynucleotidyl transferase dUTP nick end labeling (TUNEL) staining images (*E*) and quantifications (*F*) indicative of cell death in human lung slices exposed to CSE (6% for 24 h) *in vitro*. Representative TUNEL-positive cells (*green color*) are indicated by *white arrows* and magnified in the smaller window in *E*. Eto: 100 μM, 24 h. Hematoxylin and eosin (H&E) and TUNEL (*G*) staining images and quantifications of TUNEL-positive cells (*H*) in murine lung sections from wild-type C57BL/6 mice exposed to CS for 1 month. Eto: 25 mg/kg, every other day intraperitoneal injection. The number of mice is indicated by the number inside each column in *H*. (*A*, *B*, and *D*) Means ± SD from at least three biological repeats. (*F*) Means ± SEM from eight random views in each lung section. (*H*) Means ± SEM from four mice in each group and four random views in each mouse. *Scale bars*: 500 μm in *upper panels* of *G* and 100 μm in *lower panels* of *G*. $^{*}P < 0.05$, $^{**}P < 0.01$.

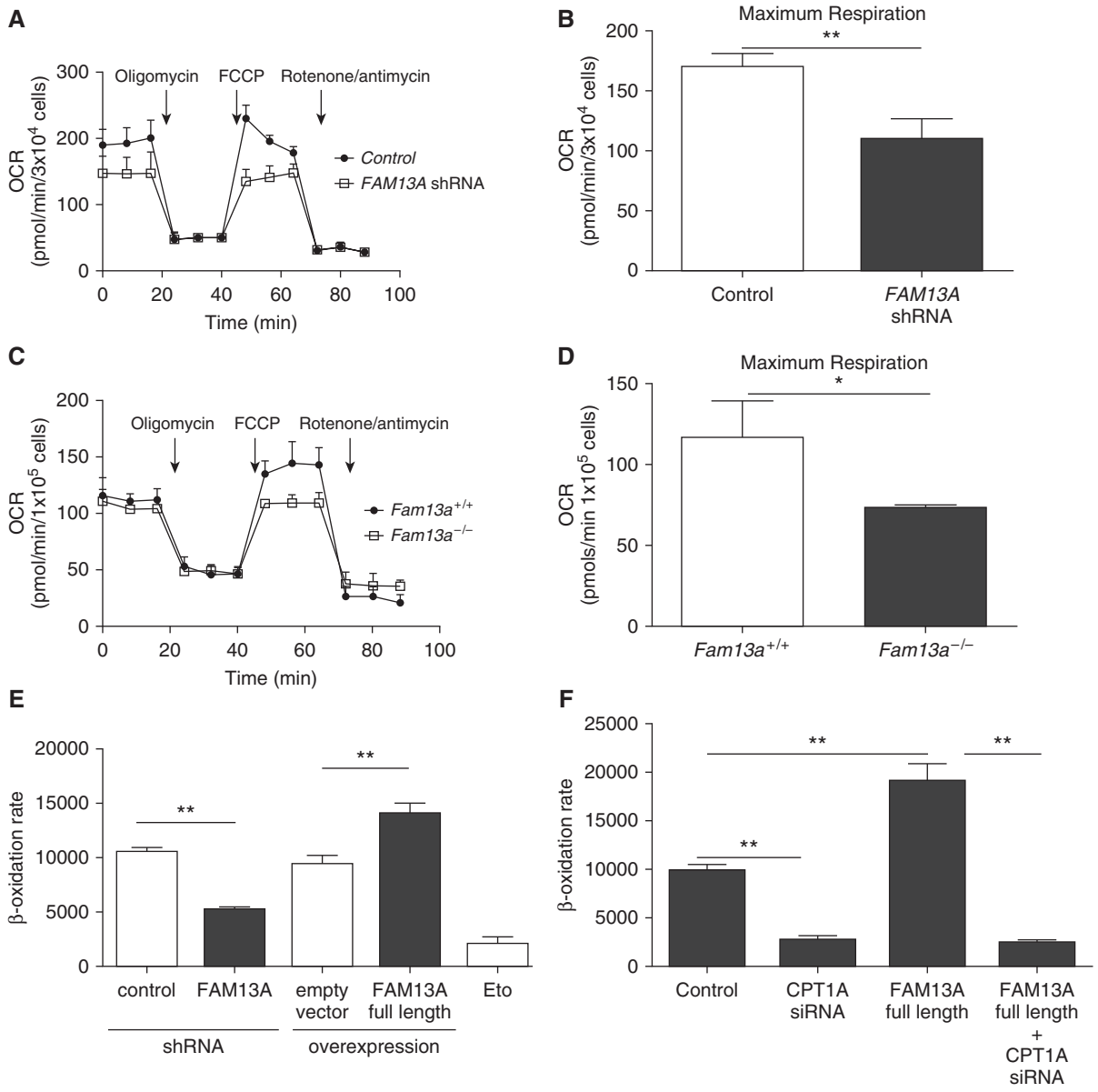

Figure 3. FAM13A (family with sequence similarity 13 member A) promotes maximal mitochondrial respiration. (*A* and *B*) OCR measurements by Seahorse assay in 16HBE cells stably infected with FAM13A short hairpin RNA (shRNA). The maximum respiration is shown in *B*. Means ± SD are from triplicate wells in one representative experiment from three biological repeats. (*C* and *D*) Mitochondrial respiration measurements in primary lung epithelial cells isolated from distal lungs of *Fam13a*$^{-/-}$ mice and their wild-type littermates (*Fam13a*$^{+/+}$). The maximum respiration is shown in *D*. Means ± SD from triplicate wells of murine lung epithelial cells from two mice/genotype. (*E*) FAO measurements in 16HBE cells stably infected with control or FAM13A shRNA or transfected with full length of FAM13A. (*F*) FAO measurements in 16HBE cells transfected with CPT1A siRNA and/or overexpressing human FAM13A. Means ± SD from triplicate wells in one representative experiment from three biological repeats. *$P < 0.05$, **$P < 0.01$.

Wnt pathway, by interacting with the protein phosphatase 2A (PP2A)/glycogen synthase kinase 3β (GSK-3β) complex (21). It was also reported that the canonical Wnt pathway promotes FAO in hepatic cells (29). Therefore, we assessed whether activation of the β-catenin/Wnt pathway regulates FAO in HBE cell lines. Surprisingly, FAO showed no changes in 16HBE cells treated with lithium chloride (5 mM), an activator of the canonical Wnt pathway associated with accumulation of β-catenin (Figure E9A). Furthermore, FAO remained at lower levels in 16HBE cells transfected with CPT1A siRNA despite lithium chloride treatment (Figure E9B). This suggested that the canonical Wnt pathway may not regulate FAO in bronchial epithelial cells, and that FAM13A may promote FAO independently of the β-catenin/Wnt pathway in bronchial epithelial cells.

Among the cellular partners of human FAM13A we previously identified by mass spectrometry (21), sirtuin 1 (SIRT1) is the most relevant for activation of FAO through its deacetylation enzymatic activity

(30–33). Here, we found that endogenous SIRT1 was coimmunoprecipitated by FLAG-tagged FAM13A in HEK 293 cells (Figure 4A). Furthermore, silencing of FAM13A significantly reduced SIRT1 enzymatic activity by 62% in 16HBE cells (Figure 4B). These results suggested that FAM13A interacts with SIRT1 and promotes its deacetylase activity. To determine the functional impact of their interaction, we measured FAO in 16HBE cells after chemical activation or genetic

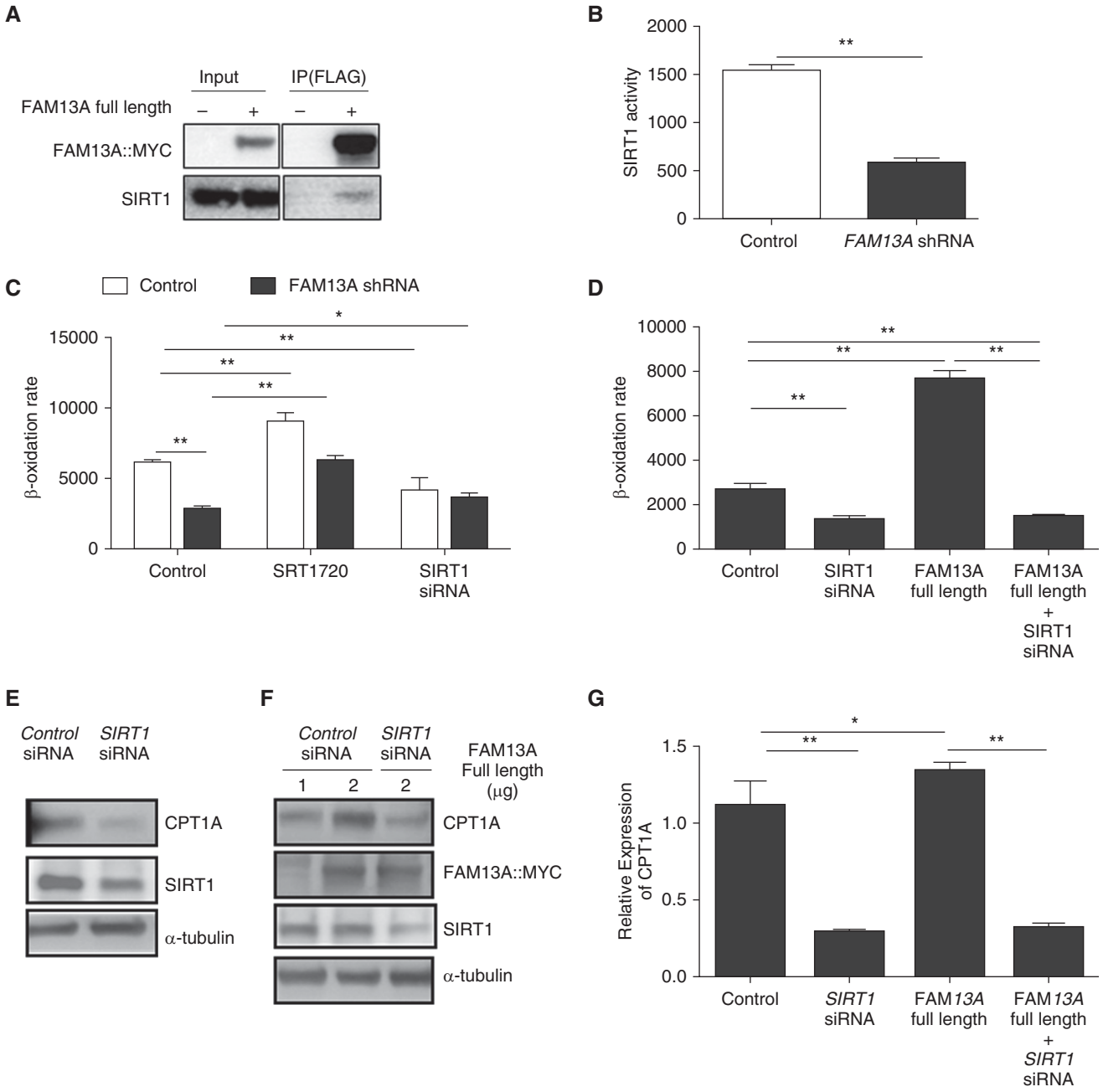

Figure 4. FAM13A interacts with sirtuin 1 (SIRT1) and promotes its deacetylation activity and expression of CPT1A. (*A*) Immunoprecipitations (IPs) with anti-Flag antibody in human embryonic kidney 293 cells transfected with Flag/Myc-tagged FAM13A followed by immunoblotting with SIRT1 antibody. (*B*) SIRT1 activity measurements in 16HBE cells infected with control or FAM13A shRNA after immunoprecipitation with SIRT1 antibody. Means ± SD from triplicate wells in one representative experiment from three biological repeats. (*C*) Measurements of FAO in 16HBE cells treated with SIRT1720 (3 μM, an activator of SIRT1) or transfected with siRNA against SIRT1. (*D*) β-oxidation measurements in 16HBE cells transfected with SIRT1 siRNA and/or Flag/Myc-tagged FAM13A. Means ± SD from triplicate wells. (*E* and *F*) Immunoblotting of CPT1A and SIRT1 in 16HBE cells transfected with SIRT1 siRNA (*E*) or cotransfected with increasing amounts of Flag/Myc tagged-FAM13A (*F*). A-tubulin was used as the loading control. (*G*) Measurements of CPT1A mRNA levels by RT-PCR in 16HBE cells transfected with SIRT1 mRNA and/or Flag/Myc-tagged FAM13A. Means ± SD from three biological repeats. $^{*}P < 0.05$, $^{**}P < 0.01$.

silencing of SIRT1. FAO significantly increased after treatment with the SIRT1 activator SRT1720 (3 μM) (34), but was reduced after silencing of SIRT1 by siRNA in 16HBE cells in the presence or absence of FAM13A (Figure 4C). Interestingly, overexpression of FAM13A failed to revert the impaired FAO due to SIRT1 silencing by SIRT1 siRNA (Figure 4D), suggesting that SIRT1 is downstream of FAM13A in regulating FAO, and FAM13A promotes FAO through SIRT1.

SIRT1 promotes FAO through transcriptional activation of multiple genes that are important for FAO, including CPT1A (35). Given that expression of CPT1A is positively regulated by FAM13A (Figure E6), we next assessed whether FAM13A promotes expression of CPT1A and FAO through SIRT1 in bronchial epithelial cells. First, the protein levels of CPT1A were reduced after SIRT siRNA transfection in 16HBE cells (Figure 4E). Second, overexpression of FAM13A increased the mRNA and protein levels of CPT1A, which was reverted by SIRT1 siRNA (Figures 4F and 4G). This suggested that SIRT1 functions downstream of FAM13A to promote transcriptional activation of CPT1A.

Loss of Fam13a Attenuates CS-Enhanced Mitochondria Respiration

We further assessed the impacts of CS exposure and *Fam13a* deficiency on the OCR in lung epithelial cells *in vivo*. We exposed age-matched *Fam13a*$^{+/+}$ and *Fam13a*$^{-/-}$ mice to CS for 1 month, and found that expression of *Cpt1a* increased in *Fam13a*$^{+/+}$ mice after 1 month of CS exposure (Figure E10A). In the meantime, we also set out to determine the impacts of FAM13A and chronic CS exposure on mitochondrial respiration *in vivo*. Primary distal lung epithelial cells were isolated and assessed for mitochondrial respiration. Maximum respiration increased by 50% in lung epithelial cells from *Fam13a*$^{+/+}$ mice after CS exposure (Figures E10B–E10F), consistent with a previous report (16). In contrast, maximum mitochondrial respiration was significantly attenuated in lung epithelial cells from both air- and CS-exposed *Fam13a*$^{-/-}$ mice compared with cells from *Fam13a*$^{+/+}$ mice. We further confirmed that the CS-induced increase of OCR was impaired in lung epithelial cells derived from *Fam13a*$^{-/-}$ mice even after 5 months of chronic CS exposure (Figures 5A and E11), suggesting that FAM13A mediates CS-induced mitochondrial respiration in distal lung epithelial cells.

Silencing of FAM13A Increases Resistance to CS-Induced Cell Death

Given that increased FAO mediates CS-induced cell death, we next assessed whether FAM13A also regulates CS-induced cell death and ROS production. First, silencing of *FAM13A* by two individual siRNAs conferred resistance to CSE-induced cell death (Figure 6A). In contrast, overexpression of human FAM13A sensitized cells to CSE-induced cell death and reverted the resistance to cell death conferred by FAM13A shRNA in 16HBE cells (Figure 6B). CSE treatment induced a 3-fold increase of intracellular ROS, which was completely attenuated upon FAM13A silencing (Figure 6C). We also detected a 4-fold increase in the number of dead cells positive for TUNEL signals in lungs from *Fam13a*$^{+/+}$ mice exposed to CS for 1 month, in contrast to a 1.64-fold increase in CS-exposed *Fam13a*$^{-/-}$ mice (Figures 6D–6F). These results suggested that FAM13A promotes CS-induced cell death *in vivo* and *in vitro*.

In summary, FAM13A promotes SIRT1 activity, increases CPT1A levels, and activates FAO. Upon CS exposure, CPT1A levels increase and FAO is activated, which mediates CS-induced ROS accumulation and cell death. Upon *Fam13a* deficiency, CPT1A levels are reduced, which attenuates CS-induced FAO and cell death (Figure 6G).

Discussion

GWASs have demonstrated a consistent association with COPD susceptibility at the *FAM13A* locus (17). Despite increasing epidemiologic evidence linking lipid metabolism to CS-induced emphysema (36, 37), whether—and if so, how—FAO, one of the major lipid metabolism pathways that are important for energy homeostasis, contributes to COPD pathogenesis has not yet been explored. Furthermore, how COPD GWAS genes determine CS-induced metabolic adaptation, as well as the biological consequences of such an adaptation, also remains enigmatic. Previously, we demonstrated that *Fam13a*$^{-/-}$ mice are resistant to CS-induced emphysema (21). Herein, we demonstrate that *FAM13A* promotes FAO by upregulating CPT1A expression, and that chemical or genetic inhibition of FAO attenuates mitochondrial-derived ROS accumulation and cell death induced by CS exposure *in vitro* and *in vivo*. Hence, we connect *FAM13A*, one of the most consistent COPD genes, to CS-induced cell death through FAO, a druggable pathway that is important for energy balance and lipid metabolism.

Emphysema, which is characterized by the destruction of alveolar walls and reduced alveolar surface areas, represents one of the major pathological changes in human COPD lungs. CS-induced ROS accumulation and epithelial cell death contribute to CS-induced emphysema, but little is known about how this happens. The mitochondrion, as the main source of intracellular ROS, is not only passively

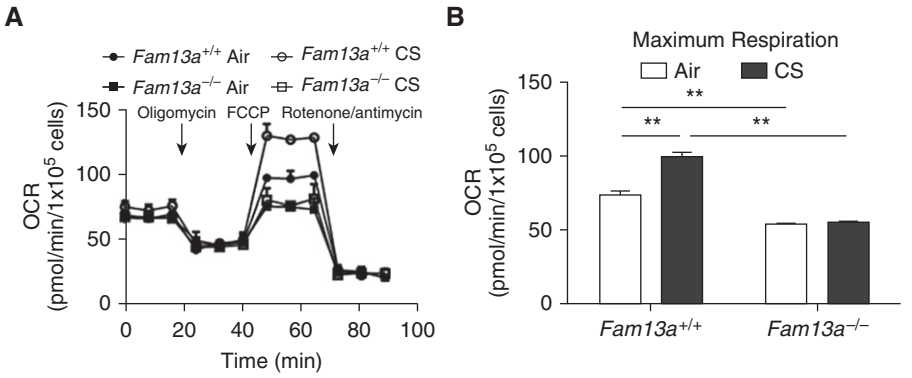

Figure 5. FAM13A-null primary lung epithelial cells demonstrated reduced mitochondrial respiration induced by CS exposure. (*A*) OCR measurements in primary alveolar epithelial cells from *Fam13a*$^{+/+}$ mice and *Fam13a*$^{-/-}$ mice exposed to 5 months of CS or air. The maximum respiration is shown in *B*. Means ± SD from triplicated wells in one assay representative of three mice in each group. $^{**}P < 0.01$.

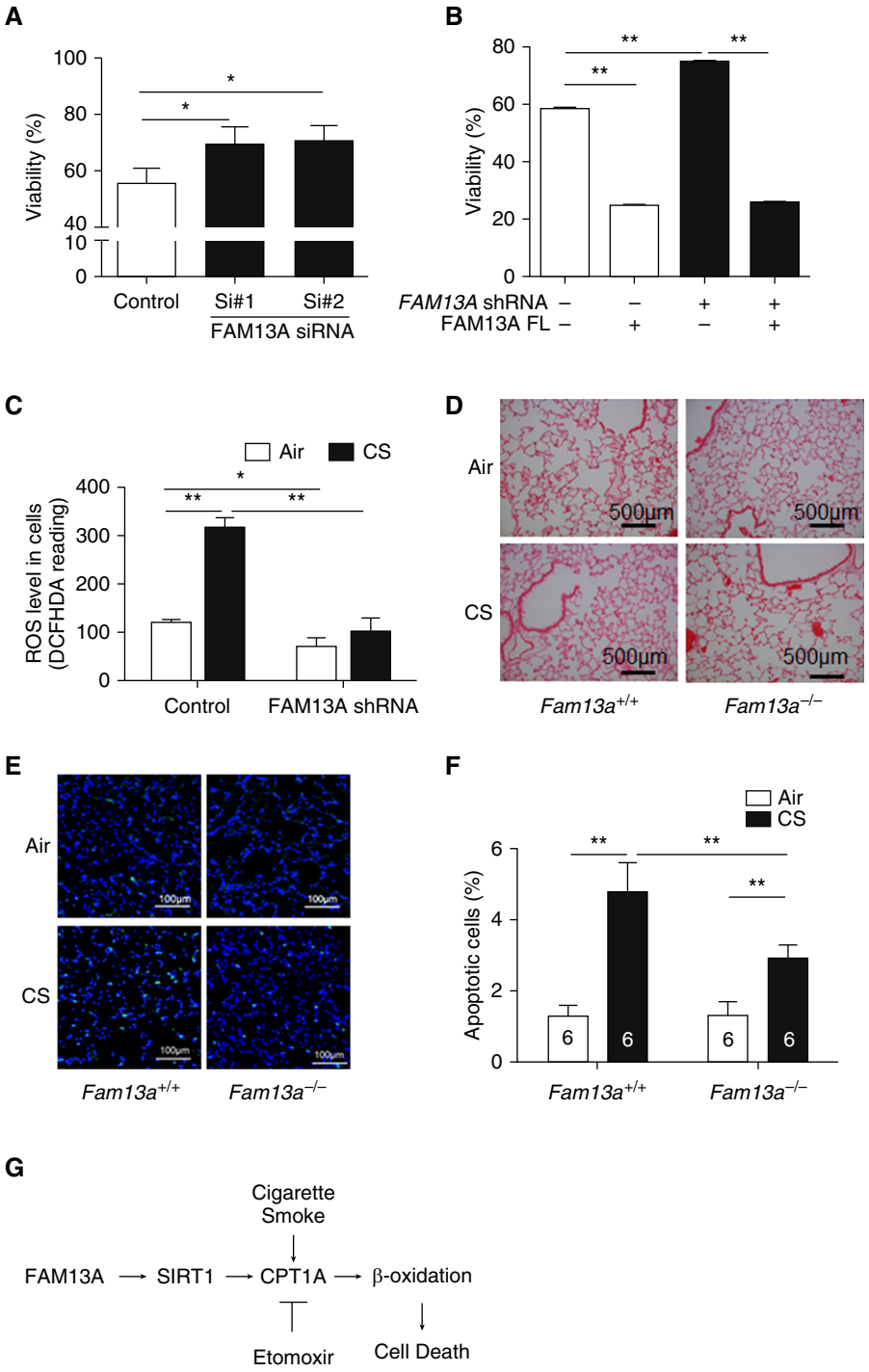

Figure 6. Silencing of FAM13A conferred resistance to CS-induced cell death. (*A*) Cell viability measurements in 16HBE cells transfected with siRNAs targeting FAM13A after CSE treatment. (*B*) Cell viability measurements in 16HBE cells stably infected with control or FAM13A shRNAs and co-transfected with or without FAM13A overexpression plasmid (FL). (*C*) Intracellular ROS measurements in 16HBE control cells or stably infected with FAM13A shRNA treated with 3% CSE for 12 h. H&E (*D*) and TUNEL (*E*) staining images and quantifications (*F*) in lungs from *Fam13a*$^{+/+}$ and *Fam13a*$^{-/-}$ mice exposed to 1 month of CS or air. (*A–C*) Means ± SD from three biological repeats. (*F*) Means ± SEM from six mice in each group and three random views in each lung sample. (*G*) Schematic illustration of the mechanism by which FAM13A promotes β-oxidation that mediates CS-induced cell death. *Scale bars*: 500 μm in panel *D* and 100 μm in panel *E*. *$P < 0.05$, **$P < 0.01$.

stressed by CS in airway epithelial cells (26) but may also actively mediate CS-induced ROS production through elevated FAO, a metabolic adaptation that occurs in response to CS exposure. Thus, the mitochondrion has been suggested as a potential therapeutic target in COPD as well as in other lung diseases (38).

Under physiological conditions, glucose is the major cellular energy source for generating ATP for various activities. However, upon CS exposure, airway epithelial cells utilize lipids to generate ATP by activation of FAO (16) (Figure 1). Direct induction of FAO by CS in airway epithelial cells may result from increased expression of CPT1A by CS. It is also possible that CS disrupts the extracellular matrix in COPD (39), and loss of extracellular-matrix attachment may promote FAO in epithelial cells (40). The change in glycolysis that occurs after CS exposure is more complicated: results from CS exposure in a murine model suggested reduced glycolysis in lung epithelial cells (16), whereas patients with COPD demonstrated faster glucose metabolism with increased glycolysis (41). Therefore, the molecular mechanism by which lung epithelial cells adapt metabolically in response to CS *in vivo* requires further investigation.

It is well accepted that chronic CS exposure in mice reduces body weight as well as fat mass (42), which may result from reduced food intake due to loss of appetite (43). Our study suggests another plausible reason for such reduced weight and fat mass after chronic CS exposure. In response to CS exposure, lung epithelial cells increased their mitochondrial respiration by enhancing FAO, which may exploit fat storage in adipose tissues to meet increased FA demands in lungs under stress conditions. Therefore, through such metabolic adaptation, lung epithelial cells are able to generate ATPs to meet their cellular energy needs. However, this metabolic adaptation works as a double-edged sword, because sustained elevation in FAO may also aggravate CS-induced ROS accumulation, mitochondrial damage, and cell death (15). This notion is supported by observations of improved cell viability and reduced mitochondrial ROS accumulation *in vitro* and *ex vivo* with Eto treatment during CS exposure (Figure 2). In addition, such continuous consumption of body fat may reduce body weight and fat mass in CS-exposed

mice. Hence, environmental CS exposure leads to a rather systematic adaption in metabolism that may in turn determine CS-induced lung injury to various degrees.

Although *FAM13A* is one of the most replicated COPD GWAS genes, little is known about its biological functions. Previously, we showed that FAM13A interacts with PP2A and promotes the degradation of β-catenin in bronchial epithelial cells (21). Therefore, increased levels of β-catenin detected in *Fam13a*$^{-/-}$ lungs may be associated with increased cell proliferation and lung repair capacity after CS-induced injury. Here, we argue that metabolic regulation may represent another complementary mechanism by which FAM13A promotes CS-induced emphysema. We found that FAM13A interacts with SIRT1, a well-known regulator of FAO. In previous studies, *Sirt*$^{+/-}$ mice showed spontaneous emphysema and SIRT1 levels were reduced in lung epithelial cells from COPD patients (44, 45). Nuclear SIRT1 activates the transcription factor forkhead box O3 (FOXO3) and thus protects cells from oxidative-stress–induced injury (44, 45). However, FAM13A mainly interacts with SIRT1 in the cytosol and promotes the deacetylation activity of cytosolic SIRT1, whose function is distinct from that of nuclear SIRT1. Cytoplasmic SIRT1 activates peroxisome proliferator-activated receptor gamma coactivator 1-α (PGC-1α) through deacetylation and increased expression of CPT1A (46, 47). FAM13A interacts with SIRT1 and induces expression of CPT1A, thereby enhancing FAO, which mediates CS-induced cell death and ROS accumulation. The promotion of FAO by FAM13A through SIRT1 may function independently of its regulation on the β-catenin/Wnt pathway but complementarily determine the susceptibility to CS-induced emphysema.

It is noteworthy that FAM13A has also been consistently associated with lung function in the general population (48), suggesting that the impact of FAM13A on lung function may not depend on smoking exposure. Consistent with this, a recent study suggested that both FAM13A and hedgehog interacting protein (HHIP) loci were significantly associated with lung-function measurements in never-smokers (49). This finding indicates that without CS exposure, an increase of FAM13A expression is sufficient to confer a risk of airway obstruction. In our experiments, we also found that overexpression of FAM13A increased the cellular FAO rate in bronchial epithelial cells independently of CS exposure (Figure 3E), and that increased FAO may predispose cells to an increased risk of cell apoptosis under CS treatment (Figure 1). However, further investigation is required to determine whether the cellular FAO rate may modulate lung function under baseline in the absence of CS exposure. If so, FAM13A may determine normal lung function maintenance through modulating lipid metabolism in lung epithelial cells.

In summary, we have shown that CS-induced metabolic adaptation, mainly activation of FAO, may contribute to CS-induced lung epithelial cell death and increase ROS accumulation, and this process is modulated by the COPD susceptibility gene, *FAM13A*. ■

Author disclosures are available with the text of this article at www.atsjournals.org.

References

1. Miniño AM, Xu J, Kochanek KD. Deaths: preliminary data for 2008. *Natl Vital Stat Rep* 2011;59:1–126.
2. Tuder RM, Petrache I. Pathogenesis of chronic obstructive pulmonary disease. *J Clin Invest* 2012;122:2749–2755.
3. Rahman I. Oxidative stress in pathogenesis of chronic obstructive pulmonary disease: cellular and molecular mechanisms. *Cell Biochem Biophys* 2005;43:167–188.
4. Tamimi A, Serdarevic D, Hanania NA. The effects of cigarette smoke on airway inflammation in asthma and COPD: therapeutic implications. *Respir Med* 2012;106:319–328.
5. Park JW, Ryter SW, Choi AM. Functional significance of apoptosis in chronic obstructive pulmonary disease. *COPD* 2007;4:347–353.
6. Chen ZH, Lam HC, Jin Y, Kim HP, Cao J, Lee SJ, Ifedigbo E, Parameswaran H, Ryter SW, Choi AM. Autophagy protein microtubule-associated protein 1 light chain-3B (LC3B) activates extrinsic apoptosis during cigarette smoke-induced emphysema. *Proc Natl Acad Sci USA* 2010;107:18880–18885.
7. Aravamudan B, Thompson MA, Pabelick CM, Prakash YS. Mitochondria in lung diseases. *Expert Rev Respir Med* 2013;7:631–646.
8. Ali Assad N, Sood A. Leptin, adiponectin and pulmonary diseases. *Biochimie* 2012;94:2180–2189.
9. Koršić M, Kušec V. Serum leptin and skeletal differences between obese and non-obese patients with chronic obstructive pulmonary disease. *Obes Facts* 2014;7:399–407.
10. Oh YM, Jeong BH, Woo SY, Kim SY, Kim H, Lee JH, Lim SY, Rhee CK, Yoo KH, Lee JH, *et al*.; KOLD Study Group. Association of plasma adipokines with chronic obstructive pulmonary disease severity and progression. *Ann Am Thorac Soc* 2015;12:1005–1012.
11. Telenga ED, Hoffmann RF, Ruben t'Kindt, Hoonhorst SJ, Willemse BW, van Oosterhout AJ, Heijink IH, van den Berge M, Jorge L, Sandra P, *et al*. Untargeted lipidomic analysis in chronic obstructive pulmonary disease. Uncovering sphingolipids. *Am J Respir Crit Care Med* 2014; 190:155–164.
12. Vernooy JH, Bracke KR, Drummen NE, Pauwels NS, Zabeau L, van Suylen RJ, Tavernier J, Joos GF, Wouters EF, Brusselle GG. Leptin modulates innate and adaptive immune cell recruitment after cigarette smoke exposure in mice. *J Immunol* 2010;184: 7169–7177.
13. Yang SY, He XY. Molecular mechanisms of fatty acid β-oxidation enzyme catalysis. *Adv Exp Med Biol* 1999;466:133–143.
14. Moczulski D, Majak I, Mamczur D. An overview of β-oxidation disorders. *Postepy Hig Med Dosw (Online)* 2009;63:266–277.
15. Rosca MG, Vazquez EJ, Chen Q, Kerner J, Kern TS, Hoppel CL. Oxidation of fatty acids is the source of increased mitochondrial reactive oxygen species production in kidney cortical tubules in early diabetes. *Diabetes* 2012;61:2074–2083.
16. Agarwal AR, Yin F, Cadenas E. Short-term cigarette smoke exposure leads to metabolic alterations in lung alveolar cells. *Am J Respir Cell Mol Biol* 2014;51:284–293.
17. Cho MH, Boutaoui N, Klanderman BJ, Sylvia JS, Ziniti JP, Hersh CP, DeMeo DL, Hunninghake GM, Litonjua AA, Sparrow D, *et al*. Variants in FAM13A are associated with chronic obstructive pulmonary disease. *Nat Genet* 2010;42:200–202.
18. Soler Artigas M, Loth DW, Wain LV, Gharib SA, Obeidat M, Tang W, Zhai G, Zhao JH, Smith AV, Huffman JE, *et al*. Genome-wide association and large-scale follow up identifies 16 new loci influencing lung function. *Nat Genet* 2011;43:1082–1090.
19. Cho MH, McDonald ML, Zhou X, Mattheisen M, Castaldi PJ, Hersh CP, Demeo DL, Sylvia JS, Ziniti J, Laird NM, *et al*.; NETT Genetics, ICGN, ECLIPSE and COPDGene Investigators. Risk loci for chronic obstructive pulmonary disease: a genome-wide association study and meta-analysis. *Lancet Respir Med* 2014;2:214–225.
20. Corvol H, Hodges CA, Drumm ML, Guillot L. Moving beyond genetics: is FAM13A a major biological contributor in lung physiology and chronic lung diseases? *J Med Genet* 2014;51:646–649.
21. Jiang Z, Lao T, Qiu W, Polverino F, Gupta K, Guo F, Mancini JD, Naing ZZ, Cho MH, Castaldi PJ, *et al*. A chronic obstructive pulmonary disease susceptibility gene, FAM13A, regulates protein stability of β-catenin. *Am J Respir Crit Care Med* 2016;194:185–197.

22. Willer CJ, Schmidt EM, Sengupta S, Peloso GM, Gustafsson S, Kanoni S, Ganna A, Chen J, Buchkovich ML, Mora S, *et al*.; Global Lipids Genetics Consortium. Discovery and refinement of loci associated with lipid levels. *Nat Genet* 2013;45:1274–1283.
23. Shungin D, Winkler TW, Croteau-Chonka DC, Ferreira T, Locke AE, Mägi R, Strawbridge RJ, Pers TH, Fischer K, Justice AE, *et al*.; ADIPOGen Consortium; CARDIOGRAMplusC4D Consortium; CKDGen Consortium; GEFOS Consortium; GENIE Consortium; GLGC; ICBP; International Endogene Consortium; LifeLines Cohort Study; MAGIC Investigators; MuTHER Consortium; PAGE Consortium; ReproGen Consortium. New genetic loci link adipose and insulin biology to body fat distribution. *Nature* 2015;518: 187–196.
24. Liu S, Brown JD, Stanya KJ, Homan E, Leidl M, Inouye K, Bhargava P, Gangl MR, Dai L, Hatano B, *et al*. A diurnal serum lipid integrates hepatic lipogenesis and peripheral fatty acid use. *Nature* 2013;502: 550–554.
25. Nemoto S, Fergusson MM, Finkel T. SIRT1 functionally interacts with the metabolic regulator and transcriptional coactivator PGC-1β. *J Biol Chem* 2005;280:16456–16460.
26. Mizumura K, Cloonan SM, Nakahira K, Bhashyam AR, Cervo M, Kitada T, Glass K, Owen CA, Mahmood A, Washko GR, *et al*. Mitophagy-dependent necroptosis contributes to the pathogenesis of COPD. *J Clin Invest* 2014;124:3987–4003.
27. Aven L, Paez-Cortez J, Achey R, Krishnan R, Ram-Mohan S, Cruikshank WW, Fine A, Ai X. An NT4/TrkB-dependent increase in innervation links early-life allergen exposure to persistent airway hyperreactivity. *FASEB J* 2014;28:897–907.
28. Bartalesi B, Cavarra E, Fineschi S, Lucattelli M, Lunghi B, Martorana PA, Lungarella G. Different lung responses to cigarette smoke in two strains of mice sensitive to oxidants. *Eur Respir J* 2005;25: 15–22.
29. Lehwald N, Tao GZ, Jang KY, Papandreou I, Liu B, Liu B, Pysz MA, Willmann JK, Knoefel WT, Denko NC, *et al*. β-Catenin regulates hepatic mitochondrial function and energy balance in mice. *Gastroenterology* 2012;143:754–764.
30. Feige JN, Lagouge M, Canto C, Strehle A, Houten SM, Milne JC, Lambert PD, Mataki C, Elliott PJ, Auwerx J. Specific SIRT1 activation mimics low energy levels and protects against diet-induced metabolic disorders by enhancing fat oxidation. *Cell Metab* 2008;8:347–358.
31. Rodgers JT, Lerin C, Haas W, Gygi SP, Spiegelman BM, Puigserver P. Nutrient control of glucose homeostasis through a complex of PGC-1α and SIRT1. *Nature* 2005;434: 113–118.
32. Gastaldi G, Russell A, Golay A, Giacobino JP, Habicht F, Barthassat V, Muzzin P, Bobbioni-Harsch E. Upregulation of peroxisome proliferator-activated receptor gamma coactivator gene (PGC1A) during weight loss is related to insulin sensitivity but not to energy expenditure. *Diabetologia* 2007;50: 2348–2355.
33. Finck BN, Gropler MC, Chen Z, Leone TC, Croce MA, Harris TE, Lawrence JC Jr, Kelly DP. Lipin 1 is an inducible amplifier of the hepatic PGC-1α/PPARα regulatory pathway. *Cell Metab* 2006;4: 199–210.
34. Milne JC, Lambert PD, Schenk S, Carney DP, Smith JJ, Gagne DJ, Jin L, Boss O, Perni RB, Vu CB, *et al*. Small molecule activators of SIRT1 as therapeutics for the treatment of type 2 diabetes. *Nature* 2007; 450:712–716.
35. Thakran S, Sharma P, Attia RR, Hori RT, Deng X, Elam MB, Park EA. Role of sirtuin 1 in the regulation of hepatic gene expression by thyroid hormone. *J Biol Chem* 2013;288:807–818.
36. Lundström SL, Balgoma D, Wheelock AM, Haeggström JZ, Dahlén SE, Wheelock CE. Lipid mediator profiling in pulmonary disease. *Curr Pharm Biotechnol* 2011;12:1026–1052.
37. Zehethofer N, Bermbach S, Hagner S, Garn H, Müller J, Goldmann T, Lindner B, Schwudke D, König P. Lipid analysis of airway epithelial cells for studying respiratory diseases. *Chromatographia* 2015;78: 403–413.
38. Agrawal A, Mabalirajan U. Rejuvenating cellular respiration for optimizing respiratory function: targeting mitochondria. *Am J Physiol Lung Cell Mol Physiol* 2016; 310:L103–L113.
39. Shapiro SD, Ingenito EP. The pathogenesis of chronic obstructive pulmonary disease: advances in the past 100 years. *Am J Respir Cell Mol Biol* 2005;32:367–372.
40. Schafer ZT, Grassian AR, Song L, Jiang Z, Gerhart-Hines Z, Irie HY, Gao S, Puigserver P, Brugge JS. Antioxidant and oncogene rescue of metabolic defects caused by loss of matrix attachment. *Nature* 2009;461:109–113.
41. Módis K, Gero D, Erdélyi K, Szoleczky P, DeWitt D, Szabo C. Cellular bioenergetics is regulated by PARP1 under resting conditions and during oxidative stress. *Biochem Pharmacol* 2012;83:633–643.
42. Chen H, Hansen MJ, Jones JE, Vlahos R, Anderson GP, Morris MJ. Detrimental metabolic effects of combining long-term cigarette smoke exposure and high-fat diet in mice. *Am J Physiol Endocrinol Metab* 2007;293:E1564–E1571.
43. Chen H, Vlahos R, Bozinovski S, Jones J, Anderson GP, Morris MJ. Effect of short-term cigarette smoke exposure on body weight, appetite and brain neuropeptide Y in mice. *Neuropsychopharmacology* 2005;30:713–719.
44. Yao H, Sundar IK, Ahmad T, Lerner C, Gerloff J, Friedman AE, Phipps RP, Sime PJ, McBurney MW, Guarente L, *et al*. SIRT1 protects against cigarette smoke-induced lung oxidative stress via a FOXO3-dependent mechanism. *Am J Physiol Lung Cell Mol Physiol* 2014; 306:L816–L828.
45. Yao H, Chung S, Hwang JW, Rajendrasozhan S, Sundar IK, Dean DA, McBurney MW, Guarente L, Gu W, Rönty M, *et al*. SIRT1 protects against emphysema via FOXO3-mediated reduction of premature senescence in mice. *J Clin Invest* 2012;122: 2032–2045.
46. Brenmoehl J, Hoeflich A. Dual control of mitochondrial biogenesis by sirtuin 1 and sirtuin 3. *Mitochondrion* 2013;13:755–761.
47. Gerhart-Hines Z, Rodgers JT, Bare O, Lerin C, Kim SH, Mostoslavsky R, Alt FW, Wu Z, Puigserver P. Metabolic control of muscle mitochondrial function and fatty acid oxidation through SIRT1/PGC-1α. *EMBO J* 2007;26:1913–1923.
48. Hancock DB, Eijgelsheim M, Wilk JB, Gharib SA, Loehr LR, Marciante KD, Franceschini N, van Durme YM, Chen TH, Barr RG, *et al*. Meta-analyses of genome-wide association studies identify multiple loci associated with pulmonary function. *Nat Genet* 2010;42:45–52.
49. van der Plaat DA, de Jong K, Lahousse L, Faiz A, Vonk JM, van Diemen CC, Nedeljkovic I, Amin N, Brusselle GG, Hofman A, *et al*. Genome-wide association study on the FEV1/FVC ratio in never-smokers identifies HHIP and FAM13A. *J Allergy Clin Immunol* 2016;139: 533–540.